System design of a pulsed laser rangefinder

H. N. Burns
H. N. Burns Engineering Corporation
1688 Wingspan Way
Winter Springs, Florida 32708

C. G. Christodoulou
University of Central Florida
Electrical Engineering Department
Orlando, Florida 32816

Glenn D. Boreman, MEMBER SPIE
University of Central Florida
Center for Research in Electro-Optics
and Lasers and Electrical
Engineering Department
Orlando, Florida 32816

Abstract. A pulsed GaAs laser rangefinder is analyzed and designed. Expressions for background and signal power, noise, and signal-to-noise ratio are derived. The effects of pulse rise time, receiver bandwidth, and SNR on probability of detection and range accuracy are discussed. A computer simulation is used to optimize laser power, receiver aperture, and preamplifier bandwidth. A method of threshold detection is presented and discussed. Experimental results include receiver preamplifier transfer function and threshold detector performance.

Subject terms: laser rangefinders; optical receivers.

Optical Engineering 30(3), 323-329 (March 1991).

CONTENTS

1. INTRODUCTION

Pulsed laser rangefinders are widely used today in a variety of remote sensing applications, including terrestrial, marine, and space target tracking and ranging, airborne altimeters, collision avoidance, terrain mapping, and surveillance.

Several new medium range applications require refinements to the state of the art. Laser rangefinders for submunition guidance,[1] remotely piloted vehicles (RPVs), and laser "tapemeasures" require high pulse repetition frequencies (PRFs) and high accuracy and resolution. Obviously, size, weight, cost, and complexity must also be minimized.

Paper 2849 received Dec. 14, 1989; revised manuscript received Oct. 11, 1990; accepted for publication Oct. 28, 1990.

This paper seeks to present a methodical approach for the system design of a high performance pulsed laser rangefinder (LRF) receiver. Results of the system analysis have been incorporated into a computer simulation that is used to optimize laser power, receiver bandwidth, and aperture. Finally, a method of implementing a practical thresholding circuit is presented.

2. PULSED RANGEFINDER SYSTEM

2.1. System block diagram

A system block diagram for a general pulsed laser rangefinder is shown in Fig. 1. The system timer, item (1), sets the PRF by generating a start pulse T_0 periodically. The start pulse triggers the pulsed laser source (2) and also initializes the range counter (8). The transmitter objective lens (3) collimates the laser beam, which propagates at the speed of light toward the target. A portion of the reflected laser beam is collected by the receiver objective lens (5) after passing through the spectral filter (4) and is focused on the detector (6). The receiver (7) amplifies and threshold detects the detector output signal and clocks the range counter with a stop pulse R_x when a valid laser return pulse is sensed. The range counter converts the time between signals T_0 and R_x to distance and displays or transmits this information.

2.2. System performance requirements

The requirements for a typical laser rangefinder will be used for this analysis. Typical performance requirements are as follows: minimum range 50 ft, maximum range 500 ft, range resolution < 1 ft, PRF 10 kHz.

A GaAs semiconductor laser (center wavelength of 904 nm) is assumed for the purpose of this analysis. The optics are assumed to be focused at infinity.

3. RADIOMETRY

3.1. Background power

The geometry of a typical submunition guidance laser rangefinder optical path is shown in Fig. 2. The background flux

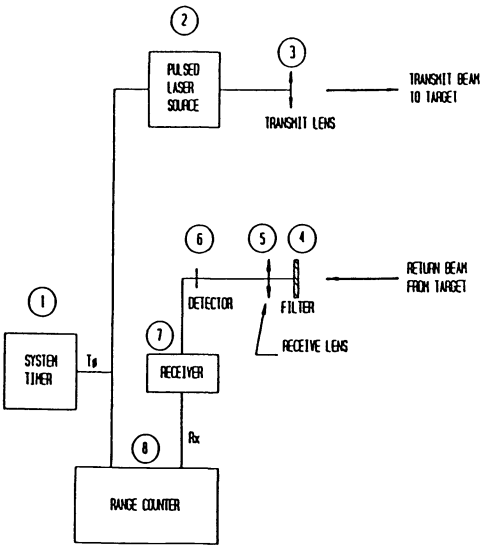

Fig. 1. System block diagram.

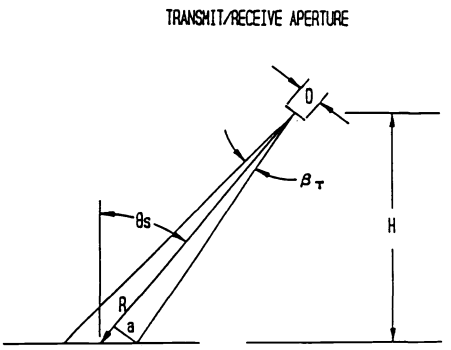

Fig. 2. Submunition guidance optical geometry.

incident on the detector, assuming a Lambertian target and ignoring diffraction effects, is given by

$$P_B = L_\lambda A_s \cos\theta_s \Omega_D \Delta_\lambda T_R \exp(-\sigma R) \quad [\mathrm{W}] \ , \tag{1}$$

where P_b is the background flux on detector [W], L_λ is the solar spectral radiance [$\mathrm{W \cdot m^{-2} \cdot \mu m^{-1} \cdot sr^{-1}}$], A_s is the detector footprint on the background [$\mathrm{m^2}$], θ_s is the angle between the target surface normal and the line joining the target and receiver centers, Ω_D is the solid angle subtended by the laser receiver aperture [sr], Δ_λ is the receiver spectral filter bandpass [μm], T_R is the transmission through the receiver optics, σ is the atmospheric extinction coefficient [$\mathrm{m^{-1}}$], and R is the slant range to the target [m].

The detector footprint A_s may be computed as

$$A_s = \frac{\pi a^2}{\cos\theta_s} \approx \frac{\pi[(\beta_R/2)R]^2}{\cos\theta_s} = \frac{\pi \beta_R^2 R^2}{4\cos\theta_s} \quad [\mathrm{m^2}] \ , \tag{2}$$

where β_R is the receiver field of view [rad]. The receiver solid angle Ω_D is given as

$$\Omega_D \approx \frac{A_R}{R^2} = \frac{\pi D_R^2}{4R^2} \ , \tag{3}$$

where D_R is the receiver clear aperture diameter [m]. The reflected solar spectral radiance L_λ is found by

$$L_\lambda = \frac{E_\lambda \rho_B}{\pi} \ , \tag{4}$$

where E_λ is the solar spectral irradiance [$\mathrm{W \cdot m^{-2} \cdot \mu m^{-1}}$] and ρ_B is the background or target reflectance. Here a narrow optical passband is assumed so that the approximation of a constant spectral irradiance function is justified. At sea level, sun at zenith, and center wavelength of 904 nm, E_λ is approximately 700 $\mathrm{W \cdot m^{-2} \cdot \mu m^{-1}}$.[2] Thus, total background power incident on the detector may be stated as

$$P_B = \frac{\pi E_\lambda \rho_B \beta_R^2 D_R^2 \Delta_\lambda T_R \exp(-\sigma R)}{16} \ . \tag{5}$$

3.2. Signal power

The geometry of the transmit laser beam is shown in Fig. 3. Here a beam filling target is assumed, and the overlap function characteristic of a binocular ranging system is ignored. Lambertian target and background are assumed.

The irradiance of the laser beam at the target/background is given by[3]

$$E_T = \frac{P_T \exp(-\sigma R)}{A_T} \quad [\mathrm{W/m^2}] \ , \tag{6}$$

where A_T is the laser footprint at the target/background [$\mathrm{m^2}$] and $P_T = P_L T_T \eta$ is the total transmitted power [W], with η being the collection efficiency of the transmit lens, P_L the raw laser peak power [W], and T_T the transmit optical path transmission. Since

$$A_T = \frac{\pi a^2}{\cos\theta_s} = \frac{\pi[(\beta_T/2)(R)]^2}{\cos\theta_s} \quad [\mathrm{m^2}] \ , \tag{7}$$

it follows that

$$E_T = \frac{4 P_L T_T \eta \cos\theta_s \exp(-\sigma R)}{\pi \beta_T^2 R^2} \quad [\mathrm{W/m^2}] \ . \tag{8}$$

Let the target exitance be denoted

$$M_T = E_T \rho_T \quad [\mathrm{W/m^2}] \ , \tag{9}$$

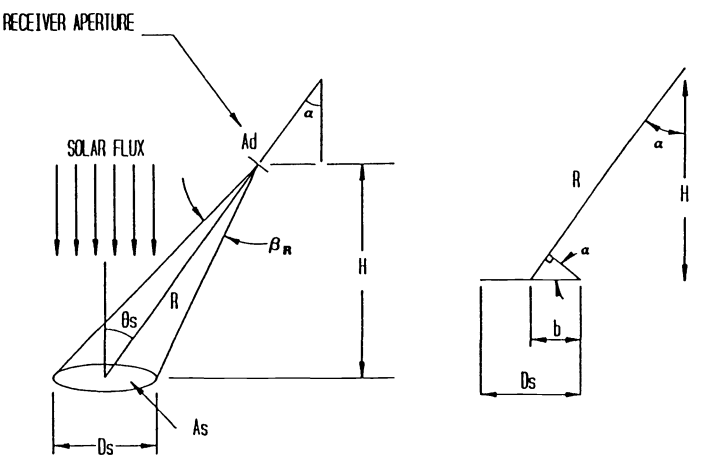

Fig. 3. Transmit laser beam geometry.

where ρ_T is the target reflectance. Then L_T, the target radiance, is given by

$$L_T = \frac{M_T}{\pi} = \frac{E_T \rho_T}{\pi} \quad [\mathrm{W \cdot m^{-2} \cdot \mu m^{-1} \cdot sr^{-1}}] \ , \tag{10}$$

or

$$L_T = \frac{4 P_L T_T \eta \cos\theta_s \exp(-\sigma R) \rho_T}{\pi^2 \beta_T^2 R^2} \ . \tag{11}$$

The peak signal power P_S incident on the detector is given by

$$P_S = L_T A_T \cos\theta_s \Omega_D T_R T_F \exp(-\sigma R) \quad [\mathrm{W}] \ , \tag{12}$$

where T_F is the receiver spectral filter transmission. Since $\Omega_D \approx \pi D_R^2 / 4R^2$, where D_R is the receiver clear aperture diameter, P_S can be expressed as

$$P_S = \frac{P_T \rho_T \cos\theta_s \pi D_R^2 T_R T_F \exp(-2\sigma R)}{4R^2} \ . \tag{13}$$

4. NOISE ANALYSIS AND SIGNAL-TO-NOISE RATIO

The primary source of noise is typically shot noise arising from solar background and signal and detector dark current. In this background-limited case, thermal noise is negligible; however, amplifier noise must be considered.

Because of its internal gain mechanism, the avalanche photodiode (APD) is superior to the pin photodiode, although the avalanche gain process itself is somewhat noisy.[4] The detector mean square noise current is given by[4,5]

$$\langle i_n^2 \rangle = 2q[I_{DS} + (I_{DB} + P_0 R_0) M^2 F] B W_N \tag{14}$$

where q is the charge on the electron [C], I_{DS} is the dark surface current (not subject to avalanche gain) [A], I_{DB} is the dark bulk current (undergoes avalanche gain) [A], $P_0 = P_S + P_B$ is the total flux incident on the detector [W], R_0 is the unity gain responsitivity [A/W], M is the avalanche gain, F is the excess noise factor, and BW_N is the noise equivalent bandwidth.

From Ref. 4, I_{DS} is typically 3×10^{-8} A/mm of detector circumference and I_{DB} is typically 1×10^{-10} A/mm^2 of detector area. The excess noise factor F is given by

$$F = 0.98\left(2 - \frac{1}{M}\right) + 0.02M \ . \tag{15}$$

The system performance, in terms of false alarm rate, probability of single pulse detection, and range error, is ultimately determined by the signal-to-noise ratio.

The electrical signal power i_s^2 is given by

$$i_s^2 = (P_s R_0 M)^2 \quad [\mathrm{A}^2] \ . \tag{16}$$

The electrical noise power i_n^2 includes shot noise, given before, plus amplifier noise:

$$i_n^2 = \{2q[I_{DS} + (I_{DB} + P_0 R_0) M^2 F] + i_{NA}^2\} B W_N \ , \tag{17}$$

where i_{NA} is the amplifier input rms noise current spectral density [A/$\sqrt{\mathrm{Hz}}$]. The signal-to-noise ratio is thus given by

$$\mathrm{SNR} = \frac{i_s^2}{i_n^2} = \frac{(P_s R_0 M)^2}{\{2q[I_{DS} + (I_{DB} + P_0 R_0) M^2 F] + i_{NA}^2\} B W_N} \ . \tag{18}$$

4.1. Calculation of minimum SNR required

A method to calculate the minimum SNR required to produce a given false alarm rate (FAR) and probability of single pulse detection (PSP) is given by Ref. 2.

A typical LRF requires a range gate (RG) of 50 ft to 500 ft, with acceptable limits on PFA (probability of false alarm) and PSP of 0.001 and 0.999, respectively. The range gate may be computed as follows:

$$\mathrm{RG} = \frac{R_{\max} - R_{\min}}{c} = 1 \ \mu\mathrm{s} \ , \tag{19}$$

where c is the speed of light. The allowable false alarm rate is given by

$$\mathrm{FAR} = \frac{\mathrm{PFA}}{\mathrm{RG}} = \frac{0.001}{1 \times 10^{-6}} = 1000/\mathrm{s} \ . \tag{20}$$

A typical GaAs laser pulse of 10 ns FWHM duration is assumed for the purposes of these calculations. Thus, $\tau \mathrm{FAR} = 1 \times 10^{-5}$, where τ is the pulse width.

From Ref. 2, for $\tau \mathrm{FAR} = 1 \times 10^{-5}$ and PSP = 0.999, a current SNR of 7.6 is required. Thus, for reliable detection, a current SNR i_s/i_n of 7.6 or power SNR i_s^2/i_n^2 of 57.76 (17.62 dB) is required.

4.2. Calculation of range error

Skolnik[6] gives the range error in terms of SNR and signal rise time. For this application, the time error is

$$\Delta t = \frac{i_n}{i_s / t_r} = \frac{\text{signal rise time}}{\text{current SNR}} \tag{21}$$

or

$$\Delta t = \frac{3 \times 10^{-9} \ \mathrm{s}}{7.6} = 3.95 \times 10^{-10} \ \mathrm{s} \ , \tag{22}$$

which converts to range error as

$$\Delta R = \left(\frac{\Delta t}{2}\right) c = \left(\frac{3.95 \times 10^{-10} \ \mathrm{s}}{2}\right)(3 \times 10^8) \ . \tag{23}$$

Thus, the worst-case range error is about 6 cm (2.3 in.), corresponding to a current SNR of 7.6 (17.6 dB). This range error is acceptable for a typical laser rangefinder application.

5. SYSTEM DESIGN

5.1. System performance simulation

The results of the previous analysis have been incorporated into a simulation program so that a parametric tradeoff analysis may be performed. The simulation is applicable to a wide variety of pulsed laser rangefinder systems, requiring only that the specific parameters for the intended application be entered into the spreadsheet.

The simulation program was used to analyze a typical submunition guidance GaAs pulsed laser rangefinder system, with the following subsystem and environment characteristics:

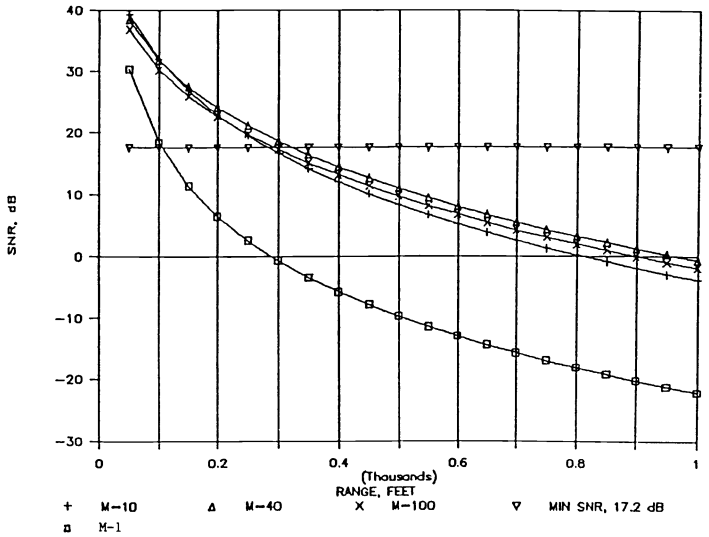

Fig. 4. Simulation results (T1). P_L = 30 W, 1 in. optics, τ_R = 3 ns.

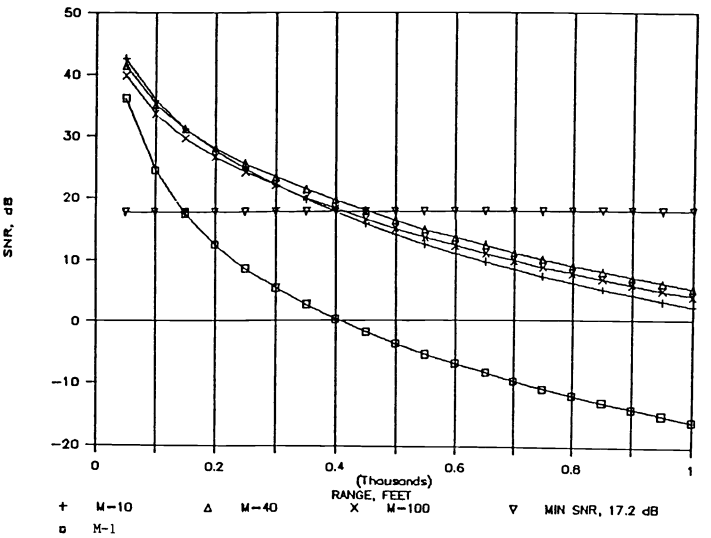

Fig. 5. Simulation results (T3). P_L = 60 W, 1 in. optics, τ_R = 3 ns.

Environment, target, background—$E_\lambda = 700\,\mathrm{W \cdot m^{-2} \cdot \mu m^{-1}}$, atmospheric extinction coefficient $\sigma = 0.12$/km, $\rho_T = 0.1$, $\rho_B = 0.6$.

Transmitter—maximum peak power $P_L = 60$ W, laser pulse rise time τ_R = ns, laser pulse width FWHM $\tau_W = 10$ ns, transmitter optics transmission factor $T_T = 0.9$, collection efficiency $\eta = 0.6$.

Receiver—$D_D = 0.0254$ m (1 in. clear aperture), $T_R = 0.9$, $T_F = 0.7$, $\beta_R = 0.009$ rad, spectral filter bandpass $\Delta_\lambda = 200$ Å.

Detector (RCA C30817 avalanche photodiode[7])—unity gain responsivity $R_0 = 0.6$ A/W, maximum avalanche gain $M = 100$, dark bulk current $I_{DB} = 0.5 \times 10^{-10}$ A, dark surface current $I_{DS} = 7.54 \times 10^{-8}$ A. These last two parameters, I_{DB} and I_{DS}, were calculated using the data for RCA 30817 APD (useful area = 0.5 mm^2, diameter = 0.8 mm).

Preamplifier—amplifier signal bandwidth $BW = 117$ MHz, noise equivalent bandwidth $BW_N = 184$ MHz, $i_n = 2.5$ pA/$\sqrt{\text{Hz}}$, amplifier transresistance $Z_T = 7.4$ kΩ.

5.2. Parametric analysis and design tradeoffs

The results of the performance simulation for $P_L = 30$ W (raw laser peak power), $\tau_R = 3$ ns, and 1 in. receiver optics are shown in Fig. 4. Clearly, the design objective of 500 ft maximum range has not been met. Depending on the avalanche gain M of the APD, the maximum effective range is limited to approximately 300 ft.

Notice that for $M = 1$ the SNR is roughly 20 dB lower than for $M = 10$ or more. This graphically demonstrates the advantage of an APD, which has an internal gain mechanism, over a pin diode for which $M = 1$. Henceforth, use of an APD is assumed, and the $M = 1$ case will no longer be considered. It should be noted, however, that for some applications the pin diode will be adequate and the use of an APD will not be warranted due to cost and circuit complexity considerations.

To meet the design objective of 500 ft maximum range, several alternatives may now be considered. The most intuitive solution is to simply increase the laser power. A 30 W laser pulse with 3 ns rise time is readily achievable. Increasing P_L to 60 W is possible, and the results, shown in Fig. 5, indicate an improvement, although the design goal still has not been met.

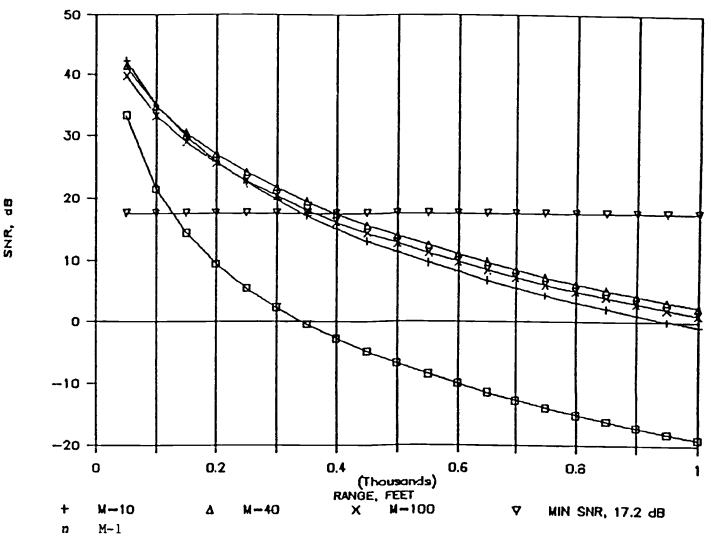

Fig. 6. Simulation results (T7). P_L = 30 W, 1 in. optics, τ_R = 6 ns.

Increasing the raw laser pulse to more than 60 W peak is not advisable since the GaAs laser source emitting area will grow due to the addition of another emitting junction. This will require a longer focal length transmitter objective lens to achieve the same transmit beam divergence, and the collection efficiency will suffer.

If the receiver objective lens clear aperture diameter is increased to 2 in., the maximum range is very nearly acceptable. If the laser power is also increased to 60 W (peak), the system performance is acceptable, with a maximum range of more than 600 ft. This solution has the disadvantage of larger size and is thus not entirely desirable.

Another design alternative is to increase the laser pulse rise time. A longer rise time requires less preamplifier bandwidth; hence, more solar background-induced shot noise is excluded. For example, if the laser pulse rise time is extended to 6 ns, only 59 MHz of signal bandwidth (92 MHz noise bandwidth) is required for a matched single pole amplifier. The effect of increasing the pulse rise time on a 30 W system is illustrated in Fig. 6. Although the maximum range goal is not met by increasing the laser pulse rise time alone, the combination of 60 W

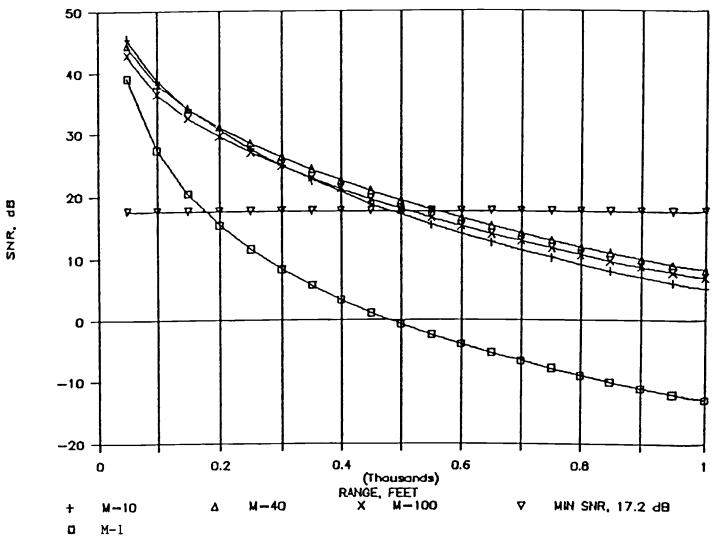

Fig. 7. Simulation results (T4). P_L = 60 W, 1 in. optics, τ_R = 6 ns.

peak power and 6 ns rise time is seen to produce the desired maximum range (Fig. 7) without the increased volume penalty associated with larger optics or laser peak power greater than 60 W.

The effect of changing the laser pulse rise time on range error must now be evaluated. From the previous section,

$$\Delta R = \left(\frac{\text{rise time}}{\text{current SNR}}\right)\left(\frac{c}{2}\right) = \left(\frac{6\times 10^{-9}}{7.6}\right)\left(\frac{3\times 10^{8}}{2}\right) = 0.1184 \text{ m} . \quad (24)$$

Thus, increasing the rise time to 6 ns increases the worst-case (i.e., at maximum range) range error to approximately 5 in. Similarly, the rise time may be further increased, if desired, to 15.4 ns, corresponding to the 1 ft maximum range error allowed for a typical laser rangefinder.

6. DETECTION

6.1. Calculation of signal dynamic range

From Eq. (13), it follows that the peak signal flux P_S incident on the detector is inversely proportional to the square of the range R. Since the range varies from 50 to 500 ft, a factor of 10, then the peak signal flux varies by 10^2 for a constant reflectance target. The target reflectance was previously modeled as $\rho_T = 0.1$ for the worst-case system analysis; however, the target reflectance can be expected to approach $\rho_T = 1$ in some cases. Hence, when the target reflectance variability is also taken into account, a signal flux variation of 1000 (60 dB) can be expected. Since signal flux [W] is converted directly to signal current [A] by the detector, the signal current dynamic range will also be 60 dB. (The above neglects the atmospheric attenuation effect, which will be discussed next.)

For the LRF designed, with APD gain $M = 40$, the simulation program indicates a peak signal current at 50 ft of 92 μA and a peak signal current at 500 ft of 0.89 μA, assuming a constant target reflectance $\rho_T = 0.1$. This corresponds to a signal dynamic range of 103.4 or 40.3 dB and includes the effect of atmospheric attenuation. Adding the 20 dB dynamic range of the target reflectance yields the worst-case return signal dynamic range of 60.3 dB. Thus, a maximum peak signal I_0 of 920 μA (for a target with $\rho_T = 1.0$ at 50 ft range) and a minimum peak signal amplitude of 0.89 μA (for a target with $\rho_T = 0.1$ at range 500 ft) are predicted by the computer simulation for the current design.

6.2. Gaussian pulse equation, given rise time

The laser pulse and detector output in a laser rangefinder are usually considered to be Gaussian in the time domain. The threshold detection process will require only the leading edge of the signal for the laser pulse time-of-flight measurement.

For a linear photodetector, the signal response to a Gaussian laser pulse has the following form:

$$I(t) = I_0 \exp\left[-2\left(\frac{t}{t_0}\right)^2\right] , \quad (25)$$

where $I(t)$ is the instantaneous signal current, I_0 is the peak signal current, and t_0 is the time from the peak signal to the point where the signal is attenuated by $1/e^2$. The rise time is defined as the time between 10% (of peak) and 90% points on the leading edge of the pulse. Consider a symmetrical Gaussian pulse, centered around $t = 0$. At the 90% point the instantaneous signal current is

$$I(t) = I_0 \exp\left[-2\left(\frac{t}{t_0}\right)^2\right] = 0.9 I_0 , \quad (26)$$

from which we obtain

$$t_{90\%} = 0.2295 t_0 , \quad (27)$$

where t_0 is the $1/e^2$. Similarly,

$$t_{10\%} = t_0\left[-\ln\left(\frac{0.1}{2}\right)\right]^{1/2} = 1.073 t_0 . \quad (28)$$

For a symmetrical Gaussian, the rise and fall times are equal. The fall time t_f may be expressed as

$$t_f = t_{10\%} - t_{90\%} = t_0(1.073 - 0.2295) \quad (29)$$

or

$$t_0 = \frac{t_f}{0.8435} = 1.186 t_r \quad (30)$$

since $t_r = t_f$. This gives the $1/e^2$ point t_0 as a function of rise time t_r.

For the purpose of this analysis, the laser pulse and corresponding detector signal current are assumed to be Gaussian in the time domain.

6.3. Constant fraction threshold detector

A simple detector may be constructed using a single high speed comparator and voltage reference, but it turns out that such a detector is inadequate for most laser rangefinders without some form of compensation being added.

Torrieri[8] suggests several alternatives as adaptive thresholding systems. The most applicable of these systems appears to be the level adjuster, or constant fraction detector (CFD). This

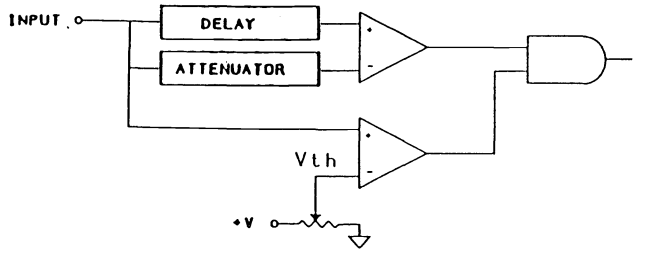

Fig. 8. Constant fraction detector block diagram.

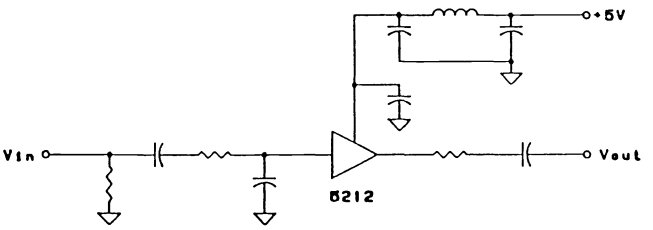

Fig. 9. Preamplifier test circuit.

threshold triggers whenever the input signal leading edge reaches a fixed fraction of the input signal amplitude. A block diagram of the CFD is depicted in Fig. 8. The key to its operation is the delay element. This enables the comparator reference voltage to be set at a fixed fraction of the signal amplitude with the signal amplitude effectively being known a priori. In this way, the CFD triggers at the same point in time on the rising edge of the signal, regardless of the amplitude of the signal.

7. EXPERIMENTAL RESULTS

7.1. Preamplifier

To determine the transfer function of the proposed preamplifier, the circuit of Fig. 9 was constructed. The 1 kΩ input resistance serves to convert the network analyzer drive voltage to a current. The 50 Ω shunt input resistor and the 33 Ω output resistor (in series with the nominally 17 Ω NE 5212 output impedance) provide impedance matching to the HP 3577A network analyzer. The measured transfer function of the NE 5212 transimpedance amplifier[9] is shown in Fig. 10.

7.2. Threshold detector

The constant fraction threshold detector proposed was constructed and tested using a programmable pulse generator and interval counter. The performance of the CFD over a widely varying range of input amplitudes is shown in Fig. 11.

8. CONCLUSIONS

The analysis of a general pulsed laser rangefinder was applied to the submunition guidance problem using a computer simulation to optimize the performance. The simulation developed herein is valid for a wide variety of similar applications, requiring only modification of the system parameters such as raw laser power, field of view, etc.

The proposed preamplifier was tested and found to have adequate bandwidth, and the constant fraction threshold detector performance was validated over a 40 dB dynamic range.

It should be mentioned here that the dynamic-range-induced errors may be further reduced by limiting the amount of dynamic range the receiver sees. The pin diode attenuators suggested by Refs. 10 and 11 appear to offer the most promise. Also, the

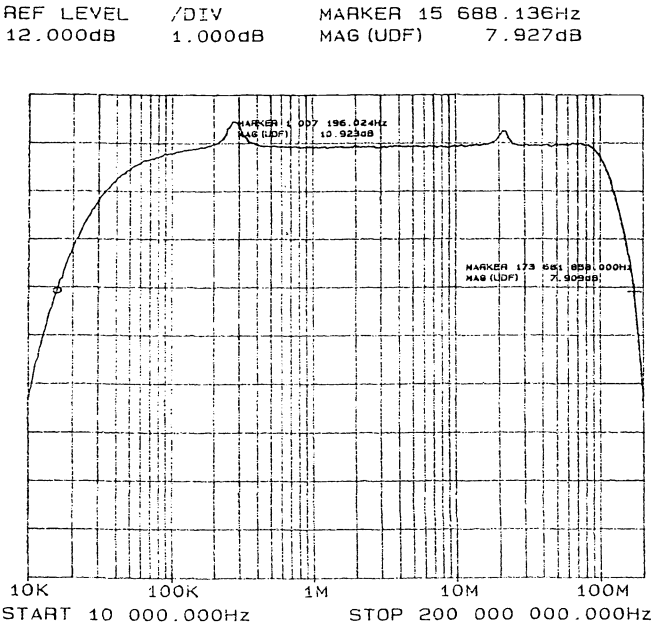

Fig. 10. Preamplifier transfer function.

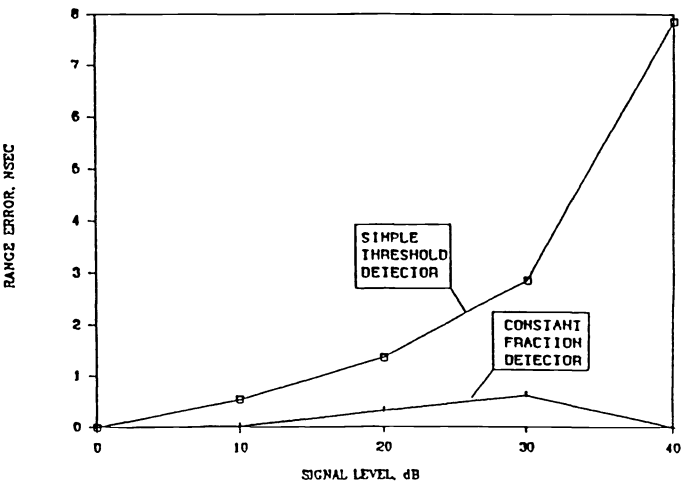

Fig. 11. Constant fraction detector performance.

dynamic range of the constant fraction detector may be increased by using an autozero circuit to reduce the voltage comparator input offset voltage.

9. REFERENCES

1. N. Huffnagle, J. Hoschette, R. Lubke, and J. Ellingboe, "Active laser sensors for submunition," Tech. Rept., Honeywell Defense Systems (Nov. 1986).
2. *Electro-Optics,* RCA Handbook (1974).
3. H. N. Burns, "Analysis and design of a pulsed GaAs rangefinder receiver," master's thesis, EE Dept., Univ. of Central Florida (1989).
4. P. E. Webb, R. J. McIntyre, and J. Conradi, "Properties of avalanche photodiodes," Tech. Rept., RCA (1977).
5. "RCA C30902 avalanche photodiode data sheet," RCA (1984).
6. M. Skolnik, *Introduction to Radar Systems,* McGraw-Hill, New York (1980).
7. "RCA C30817 avalanche photodiode data sheet," RCA (1977).
8. D. J. Torrieri, "Adaptive thresholding systems," IEEE Trans. Aerospace Electron. Syst. AES-17, 273–280 (1977).
9. "Signetics NE5212 data sheet," Signetics (1986).
10. R. Ahola and R. Myllyla, "Time-of-flight laser receiver for moving objects," IEEE Trans. Instrum. Measure. IM-35, 216–221 (1986).
11. I. Kaisto, J. Kostamovaara, M. Manninen, and R. Myllyla, "Optical rangefinder for 1.5 to 10 m distances," Appl. Opt. 21, 3258–3264 (1983).

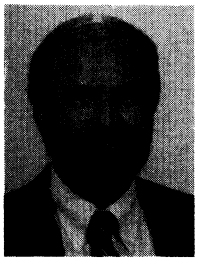

H. N. Burns is a consulting engineer specializing in the analysis and design of mechanical, electrical, and electro-optic systems. His electro-optic work includes the design of laser rangefinders, optical communication systems, and laser marking systems. Mr. Burns holds degrees in mechanical engineering (BS, University of Texas) and electrical engineering (MS, University of Central Florida) and is a registered Professional Engineer.

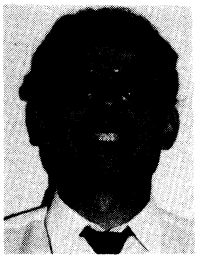

Christos G. Christodoulou was born in Cairo, Egypt, in 1955. He received the B.Sc. degree in physics and math from the American University of Cairo in 1979 and the MS and Ph.D. degrees in electrical engineering from North Carolina State University, Raleigh, in 1981 and 1985, respectively. He has been with the University of Central Florida since 1985.

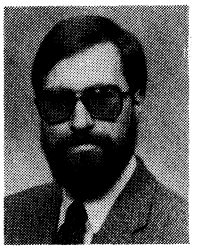

Glenn D. Boreman received the BS degree in optics from the University of Rochester in 1978 and the Ph.D. degree in optical sciences from the University of Arizona in 1984. He has held visiting technical staff positions at ITT, Texas Instruments, U.S. Army Night Vision Laboratory, and McDonnell Douglas. Dr. Boreman has been at the University of Central Florida since 1984 and is currently an associate professor of electrical engineering. He is a member of OSA, SPIE, IEEE, and SPSE and is a past president of the Florida section of OSA.